Torsional frequency response of cantilever beams immersed in viscous fluids with applications to the atomic force microscope

Christopher P. Green and John E. Sader[a)]
Department of Mathematics and Statistics, University of Melbourne, Victoria 3010, Australia

(Received 11 March 2002; accepted 12 August 2002)

The frequency response of a cantilever beam is strongly dependent on the fluid in which it is immersed. In a companion study, Sader [J. Appl. Phys. **84**, 64, (1998)] presented a theoretical model for the flexural vibrational response of a cantilever beam, that is immersed in a viscous fluid, and excited by an arbitrary driving force. Due to its relevance to applications of the atomic force microscope (AFM), we extend the analysis of Sader to the related problem of torsional vibrations, and also consider the special case where the cantilever is excited by a thermal driving force. Since longitudinal deformations of AFM cantilevers are not measured normally, combination of the present theoretical model and that of the companion study enables the complete vibrational response of an AFM cantilever beam, that is immersed in a viscous fluid, to be calculated. © *2002 American Institute of Physics.* [DOI: 10.1063/1.1512318]

I. INTRODUCTION

The frequency response of a cantilever beam can be dramatically affected by the properties of the fluid in which it is immersed, as illustrated by numerous theoretical and experimental studies.[1–11] Whereas calculation of the frequency response in vacuum can be performed routinely for many cantilever beams of practical interest,[12] analysis of the affects of immersion in fluid poses a formidable challenge. To alleviate this problem and greatly simplify the analysis, it has been commonly assumed that the fluid can be treated as being inviscid in nature.[1,2,4,7] This simplifying assumption is valid for cantilevers of macroscopic size, i.e., approximately 1 m or greater in length, where excellent agreement between theory and experiment has been demonstrated.[2]

Recently, it was established that a uniform reduction of the cantilever dimensions reduces the validity of the inviscid assumption.[3] Indeed, for cantilevers of microscopic size, such as atomic force microscope (AFM) cantilevers that are approximately 100 μm in length, fluid viscosity can greatly affect their frequency response. In Ref. 3, Sader presented a rigorous theoretical model for the frequency response of cantilever beams that are undergoing flexural vibrations and immersed in viscous fluids, which is of particular relevance to applications of the AFM.[13] A comparison of this model with detailed experimental measurements on AFM cantilevers was subsequently performed, which demonstrated the validity and accuracy of the theoretical model for cantilevers immersed in both gas and liquid.[11]

Importantly, cantilever beams also exhibit torsional and longitudinal vibrations about and along their major axis, respectively. However, a theoretical model for the frequency response of cantilever beams immersed in viscous fluids, that exhibits these modes of deformation, and knowledge and understanding of the physical processes involved, is lacking at present. This gap in the literature is particularly significant in application to the AFM, where torsional deflections are routinely measured.[14–16] Consequently, in this article we extend the analysis of Ref. 3 to account for torsional vibrations.[17] We do not consider the case of longitudinal deformations, since this cannot be measured normally in the AFM. Combining the theoretical models for flexural and torsional deformations presented here and in Ref. 3, respectively, thus enables the calculation of the complete frequency response for AFM cantilever beams immersed in viscous fluids.

We commence our investigation by examining the general case of a cantilever beam of arbitrary cross section that is excited by an arbitrary driving force. Using this general formulation, we then consider some specific cases that are of particular relevance in practice. One case we examine is that where dissipative effects can be considered small. As in Ref. 3, we rigorously prove that the analogy with the response of a simple harmonic oscillator (SHO) is valid in such cases, and we derive explicit expressions for the quality factor and resonant frequency in fluid. Importantly, we recover the well-known formula due to Chu[1] for immersion in an inviscid fluid, when the fluid viscosity is neglected. In combination with this investigation, we also present a detailed examination of a cantilever beam that is excited by a thermal driving force, i.e., by Brownian motion of the fluid molecules, since this is of fundamental importance to the AFM.[18] Detailed results are given for cantilevers with rectangular geometries and a comparison is made with the frequency response for flexural vibrations. These results are expected to be of value to the users and designers of AFM cantilevers.

II. BACKGROUND ASSUMPTIONS

We begin by reviewing the assumptions to be implemented in the present theoretical model. These assumptions are identical to those used in Ref. 3, where a more detailed discussion can be found. The problem under consideration is

a)Author to whom correspondence should be addressed; electronic mail: jsader@unimelb.edu.au

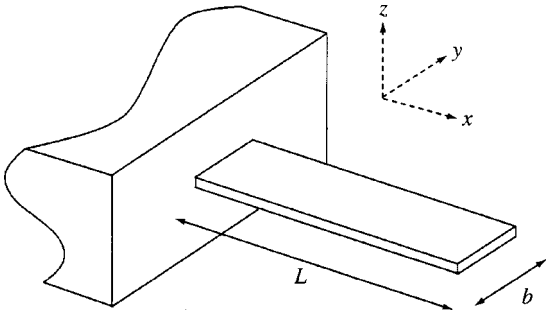

FIG. 1. Schematic illustration of a cantilever beam of rectangular cross section showing dimensions and the coordinate system. The thickness of the beam is h. The origin of the coordinate system is located at the center of mass of the cross section of the beam at its clamped end.

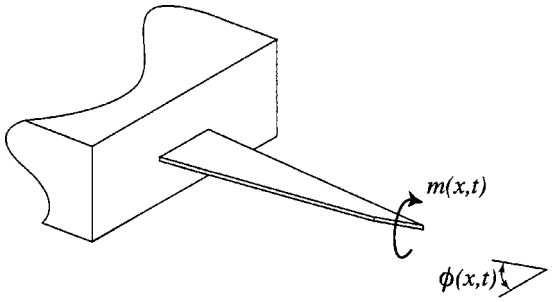

FIG. 2. Schematic illustration of a deformed cantilever beam of rectangular cross section indicating the deflection angle $\phi(x,t)$ due to an applied torque per unit length $m(x,t)$.

that of a cantilever beam vibrating in a viscous fluid. A schematic illustration of a cantilever beam of rectangular cross section is given in Fig. 1. We stress, however, that the theoretical model to be presented also holds for cantilever beams of arbitrary cross section.

In this study, we will assume the following:

(1) The cantilever beam is composed of a linearly elastic material and has a uniform cross section over its entire length;
(2) The length of the cantilever L is much greater than its width b;[19]
(3) The amplitude of torsional deflections is much smaller than any geometric length scale of the beam;[20]
(4) Internal (structural) dissipative effects in the cantilever are negligible in comparison to those in the fluid;
(5) The fluid is incompressible in nature.

All these assumptions are typically satisfied in practice.[3] Finally, we shall only consider torsional vibrations about the major axis of the cantilever.

We note that the above assumptions are also implemented in the inviscid formulation due to Chu[1] for a rectangular cantilever

$$\frac{\omega_f}{\omega_{\mathrm{vac}}}=\left(1+\frac{3\pi\rho b}{32\rho_c h}\right)^{-1/2}, \tag{1}$$

where ω_f and ω_{vac} are the torsional resonant frequencies in fluid and vacuum, respectively, ρ is the density of the fluid, ρ_c is the density of the cantilever, and b and h are the width and thickness of the cantilever, respectively. At this stage, we note that good agreement of Eq. (1) with experimental measurements on cantilevers of macroscopic size has been demonstrated previously.[2] However, as discussed above, a uniform reduction in the dimensions of the cantilever increases the effects of viscosity on the frequency response.

To examine the effect of viscosity, it is appropriate to consider the Reynolds number of the flow. Noting that the dominant length scale in the flow is the width b of the cantilever, a consequence of assumption (2), it then follows that the appropriate Reynolds number Re is[21]

$$\mathrm{Re}=\frac{\rho\omega b^2}{4\eta}, \tag{2}$$

where ρ and η are the density and viscosity of the fluid, respectively, and ω is a characteristic radial frequency of torsional vibration. Importantly, viscosity can be neglected when $\mathrm{Re}\gg 1$. For cantilevers of macroscopic size, this condition is satisfied, and explains the good experimental agreement found in Ref. 2. However, for cantilevers of microscopic size executing torsional vibrations, such as AFM cantilevers, $\mathrm{Re}\sim O(10)$. This in turn indicates that viscous effects in the fluid can be significant and should be included in any analysis.

III. THEORY

A. General theoretical model

We now present a general theoretical model for the torsional vibration of a cantilever beam immersed in a viscous fluid and excited by an arbitrary driving force.

The equation governing the deflection angle of a cantilever beam undergoing torsional deformation about its major axis is[12,17]

$$\frac{GK}{L^2}\frac{\partial^2\phi(x,t)}{\partial x^2}-\rho_c I_p\frac{\partial^2\phi(x,t)}{\partial t^2}=m(x,t), \tag{3}$$

where $\phi(x,t)$ is the deflection angle about the cantilever's major axis (see Fig. 2), G is the shear modulus of the cantilever, K is a geometric function of the cross section,[12,22,23] ρ_c its density, L its length, I_p its polar moment of inertia about the axis of rotation,[12,22] t is time, and $m(x,t)$ is the applied torque per unit length along the beam. The spatial variable x is dimensionless, having been scaled by the length of the cantilever beam, i.e., $x\in(0,1)$. The appropriate fixed-free boundary conditions for a cantilever clamped at the origin are

$$\phi(0,t)=0, \quad \left.\frac{\partial\phi}{\partial x}\right|_{x=1}=0. \tag{4}$$

Since we are primarily interested in the frequency response due to torsional vibration of the beam, we take the Fourier transform of Eq. (3) to obtain

$$\frac{GK}{L^2}\frac{d^2\Phi(x|\omega)}{dx^2}+\rho_c\omega^2 I_p\hat{\Phi}(x|\omega)=\hat{M}(x|\omega), \tag{5}$$

where the Fourier transform of any function $x(t)$ is denoted by

$$\hat{X}(\omega)=\int_{-\infty}^{\infty}x(t)e^{i\omega t}dt, \tag{6}$$

and ω is the radial frequency. The appropriate boundary conditions for $\hat{\Phi}(x|\omega)$ are the Fourier-transformed version of Eq. (4).

Next, we decompose the applied torque per unit length, $\hat{M}(x|\omega)$, into two contributions: a hydrodynamic torque per unit length, $\hat{M}_{\text{hydro}}(x|\omega)$, due to loading of the surrounding fluid, and a driving torque per unit length, $\hat{M}_{\text{drive}}(x|\omega)$, i.e.

$$\hat{M}(x|\omega)=\hat{M}_{\text{hydro}}(x|\omega)+\hat{M}_{\text{drive}}(x|\omega). \tag{7}$$

The hydrodynamic torque per unit length, $\hat{M}_{\text{hydro}}(x|\omega)$, is found by solving the Fourier-transformed equations of motion for the fluid

$$-i\omega\rho\hat{\mathbf{u}}=-\boldsymbol{\nabla}\hat{P}+\eta\boldsymbol{\nabla}^2\hat{\mathbf{u}},\quad \boldsymbol{\nabla}\cdot\hat{\mathbf{u}}=0, \tag{8}$$

where $\hat{\mathbf{u}}$ is the velocity field, $\hat{P}$ is the hydrodynamic pressure, and ρ and η are the fluid density and viscosity, respectively. The nonlinear convective inertial term is neglected in Eq. (8), a direct consequence of assumption (3) in Sec. II. Furthermore, assumption (2) in Sec. II indicates that the velocity field $\hat{\mathbf{u}}$ varies much faster over the width of beam b than it does over the length L. It is therefore clear that the velocity field at any position along a cantilever of large but finite aspect ratio (L/b) is well approximated by that for an infinitely long rigid cantilever, that is executing torsional oscillations of the same amplitude at that position. Consequently, it follows that $\hat{M}_{\text{hydro}}(x|\omega)$ has the general form

$$\hat{M}_{\text{hydro}}(x|\omega)=-\frac{\pi}{8}\omega^2\rho b^4\Gamma(\omega)(\hat{\Phi}x|\omega), \tag{9}$$

where $\Gamma(\omega)$ is the ''hydrodynamic function,'' a dimensionless complex-valued function obtained by solving Eq. (8) for motion of the rigid beam described above. The hydrodynamic function depends on the cross section of the cantilever, enabling formulation of the present model for a cantilever of arbitrary cross section. This function, which can be calculated either analytically or numerically, depending on the cross section, will be discussed in Sec. III B.

Substituting Eqs. (7) and (9) into Eq. (5), we obtain

$$\frac{d^2\hat{\Phi}(x|\omega)}{dx^2}+\frac{\rho_c\omega^2 I_p L^2}{GK}\left(1+\frac{\pi\rho b^4}{8\rho_c I_p}\Gamma(\omega)\right)\hat{\Phi}(x|\omega)=\hat{t}_{\text{drive}}(x|\omega), \tag{10}$$

where

$$\hat{t}_{\text{drive}}(x|\omega)=\frac{L^2}{GK}\hat{M}_{\text{drive}}(x|\omega) \tag{11}$$

is the scaled driving torque. Using the expression for the natural frequency of the fundamental mode of torsional vibration in vacuum,[12]

$$\omega_{\text{vac},1}=\frac{\pi}{2L}\sqrt{\frac{GK}{\rho_c I_p}}, \tag{12}$$

the elastic properties of the cantilever beam can be implicitly removed from Eq. (10) to give

$$\frac{d^2\hat{\Phi}(x|\omega)}{dx^2}+A^2(\omega)\hat{\Phi}(x|\omega)=\hat{t}_{\text{drive}}(x|\omega), \tag{13}$$

where

$$A(\omega)=\frac{\pi}{2}\frac{\omega}{\omega_{\text{vac},1}}\left(1+\frac{\pi\rho b^4}{8\rho_c I_p}\Gamma(\omega)\right)^{1/2}. \tag{14}$$

To determine the frequency response due to an arbitrary driving torque $\hat{t}_{\text{drive}}(x|\omega)$, we solve Eq. (10) using the theory of Green's functions[24] to obtain

$$\hat{\Phi}(x|\omega)=\int_0^1 G(x,x'|\omega)\hat{t}_{\text{drive}}(x'|\omega)dx', \tag{15}$$

where the appropriate Green's function is

$$G(x,x'|\omega)=-\frac{\sec[A(\omega)]}{A(\omega)}\times\begin{cases}\cos\{A(\omega)[1-x']\}\sin[A(\omega)x], & 0\leqslant x\leqslant x'\leqslant 1\\ \cos\{A(\omega)[1-x]\}\sin[A(\omega)x'], & 0\leqslant x'\leqslant x\leqslant 1\end{cases}. \tag{16}$$

Equation (15) is the required result and gives the torsional frequency response of the cantilever beam immersed in a viscous fluid and excited by an arbitrary driving force.

B. Hydrodynamic function

In order to calculate the frequency response using Eq. (15), we require an expression for the hydrodynamic function $\Gamma(\omega)$. As discussed in Sec. III A, $\Gamma(\omega)$ is obtained by solving Eq. (8) for an infinitely long rigid beam whose cross section is identical to that of the cantilever under consideration. Here, we consider two cases of practical interest, namely, cantilevers of circular and rectangular cross section.

An analytic expression for $\Gamma(\omega)$ for a beam of circular cross section is well known,[25] and is given by

$$\Gamma_{\text{circ}}(\omega)=\frac{2i}{\text{Re}}+\frac{iK_0(-i\sqrt{i\text{Re}})}{\sqrt{i\text{Re}}K_1(-i\sqrt{i\text{Re}})}, \tag{17}$$

where Re is defined in Eq. (2), b refers to the diameter of the beam and the subscript circ indicates a circular cross section. The functions K_0 and K_1 are modified Bessel functions of the third kind.[26]

Unfortunately, there does not exist an analytical expression for the hydrodynamic function of a beam of a rectangular cross section undergoing torsional oscillation. At this stage, we point out that the hydrodynamic loading on a rectangular beam of finite thickness is well approximated by that of an infinitely thin beam, provided its thickness h is much smaller than its width b. This approximation simplifies the analysis considerably and is used in the present study. Even so, formulating an analytical solution for this geometry still poses a formidable task. Therefore, to overcome this difficulty, we implement the boundary integral technique of Tuck,[27] which enables us to calculate $\Gamma(\omega)$ numerically, the results of which are presented in Fig. 3. For details of this calculation, see Appendix A.

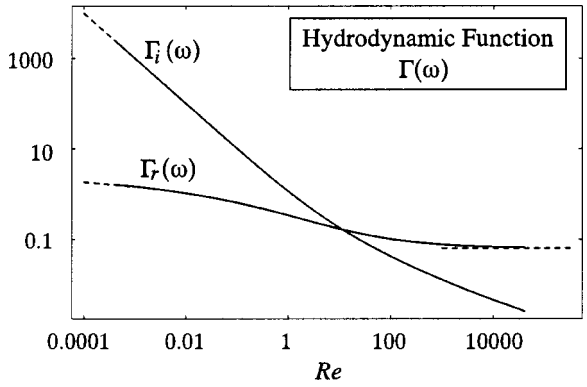

FIG. 3. Hydrodynamic function $\Gamma(\omega)$ for an infinitely thin rectangular cantilever. The subscripts r and i refer to the real and imaginary components, respectively. Asymptotic solutions are shown as dashed lines.

It is apparent from Fig. 3 that the imaginary component of $\Gamma(\omega)$ is much larger than the real component for $\mathrm{Re}\ll 1$. This contrasts to the hydrodynamic function for a rectangular beam executing flexural oscillations,[3] where the real and imaginary components of $\Gamma(\omega)$ are similar magnitude for all $\mathrm{Re}\ll 1$. This difference in behavior leads to a marked difference between the flexural and torsional frequency responses at low Re, as will be demonstrated in Sec. IV.

To validate the accuracy of this numerical solution for $\Gamma(\omega)$, and to assist in formulating an analytical expression, we now examine the low and high Re asymptotic behavior of the hydrodynamic function; the derivation of which is presented in Appendix B. These asymptotes, which are displayed as dashed lines in Fig. 3, are given by

$$\Gamma_{\mathrm{rect}}(\omega)=\begin{cases}\dfrac{i}{\mathrm{Re}}-\dfrac{3}{8}\ln(-i\sqrt{i\mathrm{Re}}), & \mathrm{Re}\to 0\\ \dfrac{1}{16}, & \mathrm{Re}\to\infty\end{cases}, \tag{18}$$

where the subscript rect refers to a beam of a rectangular cross section. Comparing this to the asymptotic behavior of $\Gamma_{\mathrm{circ}}(\omega)$ for the beam of a circular cross section,[25]

$$\Gamma_{\mathrm{circ}}(\omega)=\begin{cases}\dfrac{2i}{\mathrm{Re}}-\ln(-i\sqrt{i\mathrm{Re}}), & \mathrm{Re}\to 0\\ \sqrt{\dfrac{i}{\mathrm{Re}}}, & \mathrm{Re}\to\infty\end{cases}, \tag{19}$$

it is clear that the hydrodynamic functions for beams of rectangular and circular cross sections have similar low Re behavior, yet their asymptotic behavior for large values of Re is very different. Specifically, as $\mathrm{Re}\to\infty$, the hydrodynamic function for the beam of circular cross section goes to zero, whilst for a rectangular beam, it approaches a constant value. This contrasts to the case of flexural oscillations,[3] where the same asymptotic behavior is observed in both limits for rectangular and circular beams.

Consequently, the approximate equivalence between rectangular and circular geometries utilized in Ref. 3 in deriving an approximate analytical expression for $\Gamma(\omega)$ cannot be used here. Instead, we construct an empirical analytical formula for the hydrodynamic function for the rectangular beam, that is valid for all Re, by interpolating the numerical results presented in Fig. 3 while satisfying the appropriate asymptotic limits in Eq. (18). This is achieved using a nonlinear least-squares fitting procedure on the numerical data obtained using the boundary integral technique of Ref. 27. The resulting analytical expression for the hydrodynamic function for the rectangular beam is then given by

$$\Gamma_{\mathrm{rect}}(\omega)=\Gamma_r(\omega)+i\Gamma_i(\omega), \tag{20}$$

where

$$\begin{aligned}\Gamma_r(\omega)=&\left(\frac{5\mathrm{Re}-15\ln(\mathrm{Re})+8}{80(\mathrm{Re}+1)}\right)\times(4.179\,50-0.252\,69\tau\\&+2.883\,08\tau^2-0.086\,80\tau^3+0.338\,37\tau^4\\&+0.033\,18\tau^5+0.018\,84\tau^6)(1-2.276\,59\tau\\&+2.101\,79\tau^2-0.11365\tau^3+0.34989\tau^4\\&+0.03779\tau^5+0.01884\tau^6)^{-1},\\ \Gamma_i(\omega)=&\left(\frac{0.41}{\sqrt{\mathrm{Re}}}+\frac{1}{\mathrm{Re}}\right)\times(0.824\,94-0.677\,01\tau\\&+0.411\,50\tau^2-0.167\,48\tau^3+0.048\,97\tau^4\\&-0.011\,07\tau^5+0.001\,48\tau^6)(1-0.729\,62\tau\\&+0.406\,63\tau^2-0.165\,17\tau^3+0.049\,07\tau^4\\&-0.011\,10\tau^5+0.001\,48\tau^6)^{-1},\end{aligned} \tag{21}$$

are the real and imaginary components of the hydrodynamic function, respectively, and $\tau=\log_{10}(\mathrm{Re})$.

Although this analytical expression for $\Gamma_{\mathrm{rect}}(\omega)$ is approximate, it has the correct asymptotic behavior as $\mathrm{Re}\to 0$ and $\mathrm{Re}\to\infty$, and is accurate to within 0.1% for both the real and imaginary components over the entire range of Re shown in Fig. 3.

C. Thermal driving force

We now consider the case of a cantilever beam driven by thermal motion of the fluid molecules, and explicitly derive the thermal noise spectrum due to torsional vibrations.

First, we note that thermal excitation results in a driving torque that is stochastic in nature and independent of the spatial position x. Therefore, the driving torque can be simplified to give

$$\hat{t}_{\mathrm{drive}}(x|\omega)=\hat{t}_{\mathrm{drive}}(\omega). \tag{22}$$

Assuming the cantilever is in thermal equilibrium with its surroundings, we can then invoke the equipartition theorem, which states that the expectation value of the potential energy of each mode of torsional vibration must be equal to the thermal energy $1/2k_BT$, where k_B is Boltzmann's constant and T is the absolute temperature. This enables us to calculate the stochastic driving torques exciting each mode of the cantilever.

To proceed, we note that the deflection of the cantilever can be decomposed into the undamped modes[12]

$$\gamma_n(x)=\sin(\kappa_n x), \tag{23}$$

where $\kappa_n=(2n-1)\pi/2$, $n=1,2,...,$. Using the property that these modes form an orthogonal basis set,[28] i.e.

$$\int_0^1 \gamma_i(x)\gamma_j(x)dx=\begin{cases}\frac{1}{2}, & \text{if } i=j\\ 0, & \text{otherwise}\end{cases}, \tag{24}$$

and that each mode of vibration is driven by a stochastic torque whose magnitude is dictated by the equipartition theorem, it then follows that the rotation angle $\hat{\Phi}(x|\omega)$ can be expressed as

$$\hat{\Phi}(x|\omega)=\sum_{n=1}^{\infty}\hat{t}_n(\omega)\alpha_n(\omega)\gamma_n(x), \tag{25}$$

where

$$\alpha_n(\omega)=2\int_0^1\hat{\Phi}_0(x|\omega)\gamma_n(x)dx, \tag{26}$$

and $\hat{t}_n(\omega)$ is the stochastic driving torque for the n-th mode of vibration. The function $\hat{\Phi}_0(x|\omega)$ is obtained by solving Eq. (15) for a unit driving torque, $\hat{t}_{\text{drive}}(\omega)=1$, and is given by

$$\hat{\Phi}_0(x|\omega)=\frac{1}{A^2(\omega)}\{1-\cos[A(\omega)x] -\sin[A(\omega)x]\tan[A(\omega)]\}. \tag{27}$$

Substituting Eq. (27) into Eq. (26) and integrating, we find

$$\alpha_n(\omega)=\frac{2}{\kappa_n[A^2(\omega)-\kappa_n^2]}. \tag{28}$$

In order to apply the equipartition theorem, we need to evaluate the expectation value of the potential energy of the cantilever beam. For a beam executing torsional motion, the potential energy is given by[29]

$$U(t)=\frac{1}{2}\frac{GK}{L}\int_0^1\left(\frac{\partial\phi(x,t)}{\partial x}\right)^2dx. \tag{29}$$

Since the undamped modes form an orthogonal basis set, substituting the inverse Fourier transform of Eq. (25) into Eq. (29) gives the potential energy of the n-th mode,

$$U_n(t)=\frac{1}{2}\frac{GK}{L}\beta_n^2(t)\int_0^1\left(\frac{d\gamma_n(x)}{dx}\right)^2dx, \tag{30}$$

where $\beta_n(t)$ is the inverse Fourier transform of $\hat{t}_n(\omega)\alpha_n(\omega)$. Equating the expectation value of the potential energy of each mode $\langle U_n(t)\rangle$, with the thermal energy $1/2k_BT$, we obtain

$$\tfrac{1}{4}k_\phi\kappa_n^2\langle\beta_n^2(t)\rangle=\tfrac{1}{2}k_BT, \tag{31}$$

where k_ϕ is the torsional spring constant of the beam, defined as[22]

$$k_\phi=\frac{GK}{L}. \tag{32}$$

From the definition of $\beta_n(t)$, it then follows that:

$$\langle\beta_n^2(t)\rangle=\frac{1}{2\pi}\int_{-\infty}^{\infty}|\hat{t}_n(\omega')|_s^2|\alpha_n(\omega')|^2d\omega', \tag{33}$$

where the subscript s refers to the spectral density. Substituting Eq. (33) into Eq. (31) and solving for $|\hat{t}_n(\omega)|_s^2$ gives

$$|\hat{t}_n(\omega)|_s^2=\frac{2\pi k_BT}{k_\phi\kappa_n^2\int_0^\infty|\alpha_n(\omega')|^2d\omega'}. \tag{34}$$

Since all the vibrational modes are uncorrelated, substitution of Eq. (34) into Eq. (25) yields the required result

$$|\hat{\Phi}(x|\omega)|_s^2=\frac{2\pi k_BT}{k_\phi}\sum_{n=1}^{\infty}\frac{|\alpha_n(\omega)|^2}{\kappa_n^2\int_0^\infty|\alpha_n(\omega')|^2d\omega'}\gamma_n^2(x). \tag{35}$$

This expression is the thermal noise spectrum of the rotation angle due to excitation by Brownian motion of the fluid molecules.

In practice, deflections of AFM cantilevers are commonly measured using the optical deflection technique. Hence, the square root of Eq. (35) is directly comparable with experimental results.

D. Small dissipative effects

In the limit as dissipative effects in the fluid become small, i.e., when the real part of $A(\omega)$ is much greater than its imaginary part, the resonance peaks will be very sharp. In such cases, the thermal noise spectrum in the vicinity of the n-th resonant peak can be obtained by extracting individual terms out of the infinite series in Eq. (35), i.e.,

$$|\hat{\Phi}(x|\omega)|_s\cong\left|\frac{b_n(x)}{A^2(\omega)-\kappa_n^2}\right|, \tag{36}$$

where

$$b_n(x)=\left(\frac{8\pi k_BT}{k_\phi\kappa_n^4\int_0^\infty|\alpha_n(\omega')|^2d\omega'}\right)^{1/2}\gamma_n(x), \tag{37}$$

is a function independent of frequency ω.

From consideration of the viscous boundary layer on the surface of the beam, which forms in this limit ($\text{Re}\gg1$), it is apparent that the hydrodynamic function $\Gamma(\omega)$ varies as $O(\omega^{-1/2})$.[30] From Eq. (14), it is then clear that the function $A^2(\omega)$ is dominated by an $O(\omega^2)$ variation. Consequently, in the immediate vicinity of a resonant peak, $\Gamma(\omega)$ can be considered constant to leading order, and evaluated at the resonant frequency of the mode in the absence of dissipative effects, $\omega_{R,n}$. Generalizing $A(\omega)$ to encompass all vibrational modes, and evaluating the hydrodynamic function at the resonant frequency of the n-th mode, $\omega_{R,n}$, we obtain

$$A_n(\omega)\cong\kappa_n\left(\frac{\omega}{\omega_{\text{vac},n}}\right)\left(1+\frac{\pi\rho b^4}{8\rho_cI_p}[\Gamma_r(\omega_{R,n})+i\Gamma_i(\omega_{R,n})]\right)^{1/2}, \tag{38}$$

where $\Gamma_r(\omega_{R,n})$ and $\Gamma_i(\omega_{R,n})$ refer to the real and imaginary components of the hydrodynamic function, respectively. It then follows from Eq. (38) that in the limit of small dissipative effects, $\omega_{R,n}$ is given by

$$\frac{\omega_{R,n}}{\omega_{\text{vac},n}}=\left(1+\frac{\pi\rho b^4}{8\rho_cI_p}\Gamma_r(\omega_{R,n})\right)^{-1/2}. \tag{39}$$

Substituting this expression into Eq. (38) and rearranging, we find

$$A_n(\omega) = \kappa_n \left(\frac{\omega}{\omega_{R,n}} \right) \left(1 + \frac{i}{Q_n} \right)^{1/2}, \tag{40}$$

where

$$Q_n = \frac{\dfrac{8\rho_c I_p}{\pi \rho b^4} + \Gamma_r(\omega_{R,n})}{\Gamma_i(\omega_{R,n})}. \tag{41}$$

Substituting Eq. (40) into Eq. (36) and using the property that in the limit of small viscous effects, $\omega \cong \omega_{R,n}$ in the vicinity of a resonant peak, we obtain

$$\left| \frac{\kappa_n^2 \hat{\Phi}(x|\omega)}{\omega_{R,n}^2 b_n(x)} \right|_s \cong \left[(\omega^2 - \omega_{R,n}^2)^2 + \frac{\omega^2 \omega_{R,n}^2}{Q_n^2} \right]^{-1/2}, \tag{42}$$

which is the frequency response of a simple harmonic oscillator (SHO), with resonant frequency $\omega_{R,n}$ and quality factor Q_n, defined in Eqs. (39) and (41) respectively.

From Eq. (40), it is clear that dissipative effects in the fluid can be considered small provided $Q_n \gg 1$. In this region, the analogy with the response of a SHO is valid, which is identical to the findings for flexural vibrations.[3]

IV. RESULTS AND DISCUSSION

Due to its significance to the AFM, we now present explicit numerical results for a cantilever beam of a rectangular cross section that is excited by a thermal driving force. Throughout, we assume that the thickness h of the beam is much smaller than its width b, which is the case most often encountered in practice. Even though we only consider cantilevers with rectangular cross sections here, we emphasize that the theoretical model presented above is applicable to cantilever beams of arbitrary cross sections that are immersed in viscous fluids of arbitrary density and viscosity, and excited by arbitrary driving forces.

It is important to note that in practice, expressions for the torsional frequency response presented in the preceding sections are valid provided the mode number n is not large. This restriction arises from the assumption that the cantilever's length L greatly exceeds its width b. Consequently, we restrict our attention to the fundamental mode, and in some cases, the next harmonic.

For the rectangular beam under consideration, the geometric parameters I_P and K are well approximated by[22]

$$I_P \cong \frac{b^3 h}{12}, \quad K \cong \frac{b h^3}{3}. \tag{43}$$

It then follows from Eqs. (14), (20), and (43), that there exist two natural dimensionless parameters that characterize the problem,

$$\bar{T} = \frac{\rho b}{\rho_c h}, \quad \overline{\mathrm{Re}} = \frac{\rho \omega_{\mathrm{vac},1} b^2}{4\eta}. \tag{44}$$

Physically, the parameter $\bar{T}$ is proportional to the ratio of the added-apparent mass due to inertial forces in the fluid to the actual mass of the cantilever, in the absence of viscous effects. The other parameter $\overline{\mathrm{Re}}$ is a normalized Reynolds number, which relates the importance of inertial to viscous forces in the fluid.

Importantly, using Eqs. (12) and (43), $\overline{\mathrm{Re}}$ can be expressed in terms of the material and geometric properties of the beam

$$\overline{\mathrm{Re}} = \frac{\pi}{4} h \frac{b}{L} \frac{\rho}{\eta} \sqrt{\frac{G}{\rho_c}}. \tag{45}$$

From Eqs. (44) and (45), it is then clear that as the dimensions of the cantilever are uniformly reduced, $\bar{T}$ remains constant while $\overline{\mathrm{Re}}$ decreases linearly with the thickness h. This indicates that viscous effects in the fluid become increasingly important as the dimensions of the cantilever beam are uniformly reduced, in line with the analysis of the flexural response.[3] We present numerical results that examine the consequences of this phenomenon below.

In practice, AFM cantilevers are immersed in both gaseous and liquid mediums, and we use the parameter $\bar{T}$ to distinguish between these two cases. In gases and liquids, the values of $\bar{T}$ typically differ by three orders of magnitude, due to the difference in the density of gas relative to liquid. Consequently, for AFM cantilevers, $\bar{T} \sim O(10^{-2})$ for gases and $\bar{T} \sim O(10)$ for liquids, which are identical values to those used in the analysis of the flexural response.[3] Values of $\overline{\mathrm{Re}}$ for the torsional response, however, are typically an order of magnitude larger than the corresponding values for the flexural response. The reason for this follows from the relationship between the fundamental vacuum frequencies of flexural and torsional vibrations, which is obtained using Eq. (12) of Ref. 3 and Eq. (12) of this paper,

$$\frac{\omega_{\mathrm{vac},1}^t}{\omega_{\mathrm{vac},1}^f} = 2.1886 \frac{L}{b} \sqrt{\frac{1}{1+\nu}}, \tag{46}$$

where the superscripts t and f refer to torsional and flexural vibrations, respectively. For typical AFM cantilevers, $L/b \sim O(10)$ and $\nu \approx 0.25$. From Eq. (46), we then find that $\omega_{\mathrm{vac},1}^t \approx 10 \omega_{\mathrm{vac},1}^f$, indicating that viscosity is expected to be less important for the torsional response than for the flexural response. For AFM cantilevers undergoing torsional vibrations, we then have $\overline{\mathrm{Re}} \sim O(10)$ for gases and $\overline{\mathrm{Re}} \sim O(100)$ for liquids, values ten times larger than those for the corresponding case of flexural vibration.[3]

Importantly, in the limit as fluid viscosity becomes negligible, i.e., $\overline{\mathrm{Re}} \to \infty$, we recover the inviscid result of Chu[1] from Eqs. (18), (39) and (43), namely,

$$\frac{\omega_{R,n}}{\omega_{\mathrm{vac},n}} = \left(1 + \frac{3\pi\rho b}{32 \rho_c h} \right)^{-1/2}. \tag{47}$$

We shall examine the validity and accuracy of this inviscid model when applied to AFM cantilevers in subsequent results.

In Fig. 4, the torsional frequency response of a rectangular cantilever immersed in gas, in the vicinity of the fundamental resonant peak, is examined. From these results, it is clear that as $\overline{\mathrm{Re}}$ is decreased while $\bar{T}$ is held constant, the relative shift in the peak (resonant) frequencies from vacuum to gas increases, while the quality factor decreases. This is a

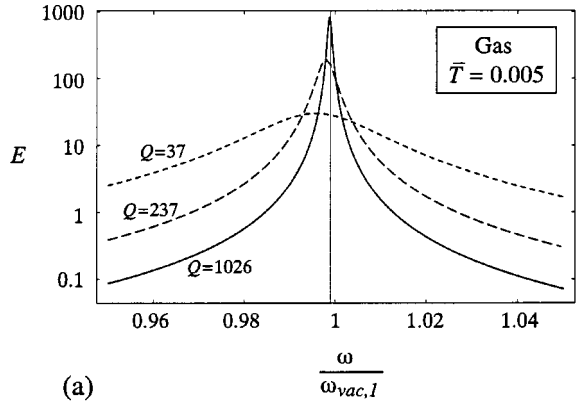

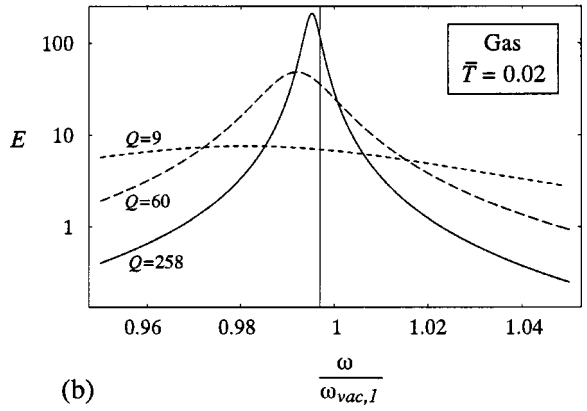

FIG. 4. Normalized thermal spectra $E=|\hat{\Phi}(1|\omega)|_s^2 k_\phi \omega_{\mathrm{vac},1}/(2k_BT)$ in the vicinity of the fundamental resonance peak for $\overline{\mathrm{Re}}=1$ (– – –); $\overline{\mathrm{Re}}=10$ (— —); and $\overline{\mathrm{Re}}=100$ (——). The vertical line is the inviscid result Eq. (47). Quality factors $Q=Q_1$, as obtained from Eq. (41) are also given. (a) $\bar{T}=0.005$ and (b) $\bar{T}=0.02$.

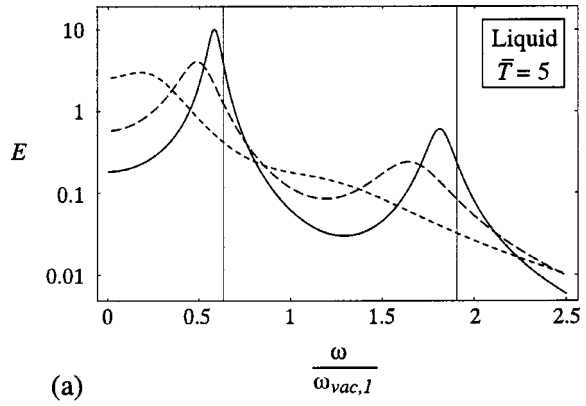

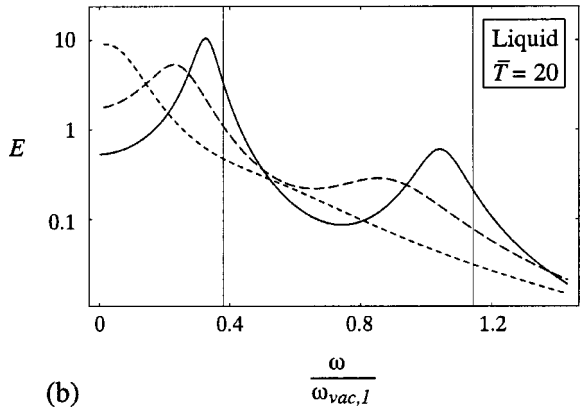

FIG. 5. Normalized thermal spectra $E=|\hat{\Phi}(1|\omega)|_s^2 k_\phi \omega_{\mathrm{vac},1}/(2k_BT)$ in the vicinity of the fundamental resonance peak for $\overline{\mathrm{Re}}=10$ (– – –); $\overline{\mathrm{Re}}=100$); and $\overline{\mathrm{Re}}=1000$ (——). The vertical lines are the inviscid results Eq. (47). (a) $\bar{T}=5$ and (b) $\bar{T}=20$.

direct consequence of the increasing effect of viscosity. In practice, this reduction in $\overline{\mathrm{Re}}$ at constant $\bar{T}$ can be realized by either a uniform decrease in the dimensions of the cantilever, or an increase in its length only. We emphasize that the shift in peak frequencies is primarily due to inertial effects in the fluid, with dissipative effects contributing comparatively little, i.e., the peak frequencies are accurately described by Eq. (39). However, comparing these results with those predicted by the inviscid model, Eq. (47), which neglects viscous effects, it is clear that the inviscid model can lead to large errors in the peak frequencies.

Turning our attention to the quality factor, it is evident from Fig. 4 of this article, and Fig. 3 of Ref. 3, that the quality factors for the torsional response are significantly larger than those of the corresponding flexural response. This finding is in line with the above prediction that viscous effects in the fluid are indeed less important for torsional vibrations.

Next, we examine the effect of immersing cantilevers in liquid. Corresponding results for the first two modes of vibration of a cantilever immersed in liquid are presented in Fig. 5. As in Fig. 4, we find that as $\overline{\mathrm{Re}}$ is decreased for a fixed $\bar{T}$, the resonance peaks shift to lower frequencies, although the shift is more pronounced due to the increased density of liquid relative to gas. We also find that the inviscid model leads to significant errors for the (typical) values of $\overline{\mathrm{Re}}$ considered. Importantly, all quantitative effects described in Ref. 3 for the flexural response are also observed here. Namely, significant coupling of the first higher harmonic and the fundamental resonance occurs as $\overline{\mathrm{Re}}$ is reduced, and the peak noise level of the fundamental mode can actually increase with a decrease in $\overline{\mathrm{Re}}$. This behavior will be examined in detail below.

To quantify the dependence of the fundamental peak frequency and quality factor on $\overline{\mathrm{Re}}$ and $\bar{T}$, we present numerical results for these quantities in Figs. 6 and 7, respectively. The peak frequency is calculated numerically from Eq. (35), whereas the quality factor is obtained directly from Eq. (41). It is evident from Fig. 6 that a decrease in $\overline{\mathrm{Re}}$ at a constant value of $\bar{T}$, or an increase in $\bar{T}$ at a constant $\overline{\mathrm{Re}}$, enhances the relative shift in the peak frequency from vacuum to fluid. Physically, the former case can be realized by uniformly decreasing all the dimensions of the cantilever, whereas the latter case corresponds to a uniform increase in the width and length at fixed thickness. We observe that the peak frequency of a cantilever immersed in a liquid is typically much smaller than that of a cantilever immersed in a gas; this is primarily a consequence of greater inertial loading in liquids. As $\overline{\mathrm{Re}} \to \infty$, the peak frequencies approach values predicted by the inviscid model, Eq. (1). Upon comparison of Fig. 6 with Fig. 5 of Ref. 3, it is clear that as $\overline{\mathrm{Re}}$ is reduced at fixed $\bar{T}$, the peak frequency of the fundamental mode decreases much more rapidly for the torsional response than for the flexural response for $\overline{\mathrm{Re}} \lesssim 1$. This is consistent with the marked dif-

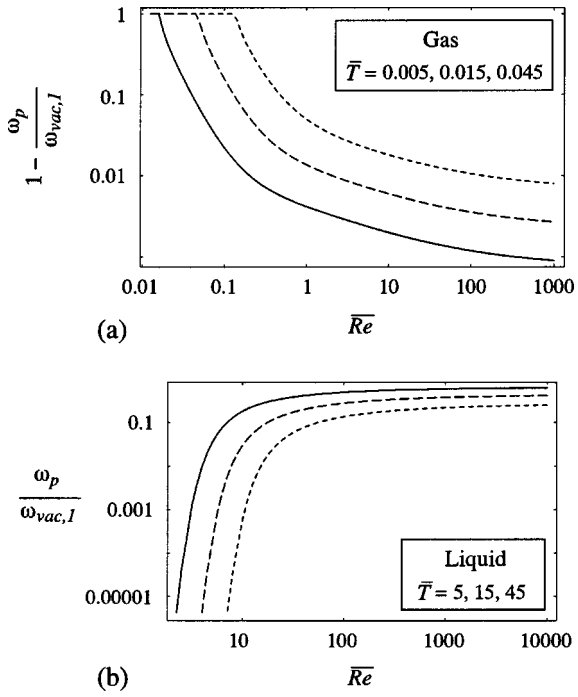

FIG. 6. Peak frequency ω_p of fundamental mode. (a) Gas: $\bar{T}=0.005$ (——); $T=0.015$ (— —); and $T=0.045$ (– – –). Inviscid results as obtained from Eq. (47) are $1-\omega_p/\omega_{\mathrm{vac},1}=0.000\,735$, 0.002 20, and 0.006 56, respectively. (b) Liquid: $T=5$ (——); $T=15$ (— —); and $T=45$ (– – –). Inviscid results are obtained from Eq. (47) are $\omega_p/\omega_{\mathrm{vac},1}=0.636$, 0.430, and 0.265, respectively.

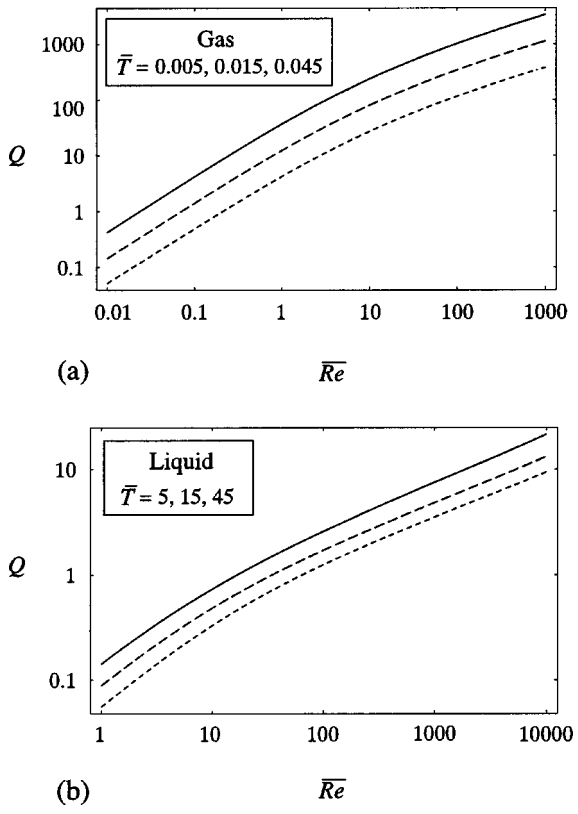

FIG. 7. Quality factor, $Q=Q_1$, of fundamental mode. (a) Gas: $\bar{T}=0.005$ (——); $T=0.015$ (— —); and $T=0.045$ (– – –). (b) Liquid: $T=5$ (——); $T=15$ (— —); and $T=45$ (– – –).

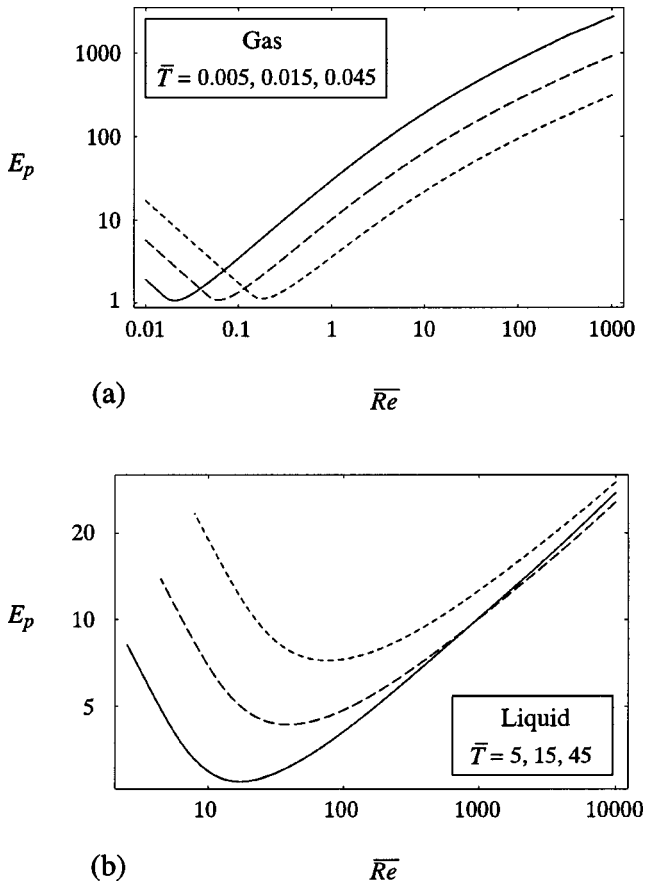

FIG. 8. Normalized peak energy $E_p=|\hat{\Phi}(1\rfloor\omega_p)|_s^2 k_\phi \omega_{\mathrm{vac},1}/(2k_BT)$ of fundamental mode. (a) Gas: $T=0.005$ (——); $T=0.015$ (— —); and $T=0.045$ (– – –). (b) Liquid: $T=5$ (——); $T=15$ (— —); and $T=45$ (– – –).

ference in the hydrodynamic functions for the two cases at small values of $\overline{\mathrm{Re}}$, as discussed in Sec. III B, c.f., Fig. 3 with Fig. 1 of Ref. 13.

The quality factors of the fundamental resonance peaks, $Q=Q_1$, obtained from Eq. (41), are presented in Fig. 7. As expected, the quality factor decreases as $\overline{\mathrm{Re}}$ is reduced at fixed T. We emphasize that these results give quantitative information about the shape of the resonant peak when $Q \gg 1$, for it is in this region that the analogy with a SHO is derived formally. For $Q \lesssim O(1)$, however, the analogy with the response of a SHO is not valid. Nonetheless, such values of Q indicate significant broadening of the resonance peaks. Finally, we note that the current model predicts a nonzero peak frequency for all values of $\overline{\mathrm{Re}}$, in line with the predictions for flexural vibrations.[3] However, the flexural resonance peaks are much sharper than the torsional peaks for $Q \lesssim O(1)$ an example of which can be seen by comparing the $\overline{\mathrm{Re}}=10$ curve in Fig. 5(b) of this article with the $\overline{\mathrm{Re}}=1$ curve in Fig. 4(b) of Ref. 3.

Due to its importance to noise considerations in AFM measurements,[8,18] we now examine the peak thermal energy of the fundamental mode of torsional vibration, the results of which are presented in Fig. 8, and have been calculated using Eq. (35). Note that there exists a distinct minimum in the peak energy. Interestingly, the value of $\overline{\mathrm{Re}}$ where this occurs coincides with a quality factor of $Q_1 \sim 1$, as calculated from

Eq. (41). This phenomenon was also observed for flexural vibrations.[3] The physical reason for this phenomenon is identical to that for flexural vibrations, and consequently the reader is referred to Ref. 3 for a detailed discussion.

In many applications, the deflections of AFM cantilevers are measured using the optical deflection technique. For such situations, the complete thermal noise spectrum of a cantilever beam, $|S_{\mathrm{comp}}(x|\omega)|_s^2$, can be obtained by summing the slope and rotation angle of flexural and torsional deflections, respectively. Using the theoretical models presented here and in Ref. 3, and assuming identical sensitivities for flexural and torsional measurements,[31] we then obtain

$$|S_{\mathrm{comp}}(x|\omega)|_s^2=\frac{3\pi k_B T}{kL^2}F(x|\omega)+\frac{2\pi k_B T}{k_\phi}P(x|\omega), \quad (48)$$

where $F(x|\omega)$ and $P(x|\omega)$ are given in Eq. (29b) of Ref. 3 and Eq. (35) of this article, respectively, and k is the normal spring constant.[3] Using Eq. (28) of Ref. 3 and Eq. (32) of this article, Eq. (48) can be reexpressed as

$$|S_{\mathrm{comp}}(x|\omega)|_s^2=\frac{3\pi k_B T}{kL^2}(F(x|\omega)+(1+\nu)P(x|\omega)). \quad (49)$$

We also define a parameter

$$\lambda=\frac{L}{b}\sqrt{\frac{1}{1+\nu}}, \quad (50)$$

which is a scaled aspect ratio that is proportional to the ratio of the vacuum frequencies of torsional and flexural vibrations, c.f., Eq. (46). This parameter will be utilized in the following discussion.

We now investigate the relationship between the peak noise levels of the fundamental resonances for flexural and torsional vibrations, i.e., the ratio of $(1+\nu)P(x|\omega_p^t)$ to $F(x|\omega_p^f)$, where ω_p^t and ω_p^f refer to the fundamental peak frequencies of the torsional and flexural modes, respectively. Results for rectangular cantilever beams immersed in gas and liquid are presented in Fig. 9, as a function of the parameters $\overline{\mathrm{Re}_f}$, $\overline{T}$, and λ. The subscript f in $\overline{\mathrm{Re}_f}$ refers to the normalized Reynolds number for flexural vibrations, which is defined in Eq. (37) of Ref. 3. Note that in all cases, the flexural peak noise level exceeds the torsional peak noise level, and this difference rises as λ is increased.

It is of interest to examine the physical significance of these results, and consider three separate cases:

(I.) *A uniform reduction in the dimensions of the cantilever,* corresponding to reducing $\overline{\mathrm{Re}_f}$ at constant $\overline{T}$ and λ;

(II.) *An increase in the length only of the cantilever,* which corresponds to reducing $\overline{\mathrm{Re}_f}$ but increasing λ at constant $\overline{T}$;

(III.) *A reduction in the width only of the cantilever,* corresponding to reducing $\overline{\mathrm{Re}_f}$ and $\overline{T}$, while increasing λ.

To examine the effects of these three cases, we introduce a geometric scaling parameter ζ, which is used to vary the dimensions of the cantilever in each case comparatively. In Case I, the dimensions are varied as $(L/\zeta, b/\zeta, h/\zeta)$, in Case II as $(\zeta L, b, h)$, whereas in Case III we have $(L, b/\zeta, h)$. Increasing the single parameter ζ, thus enables us to impose a uniform variation in all three cases, and make a simultaneous comparison.

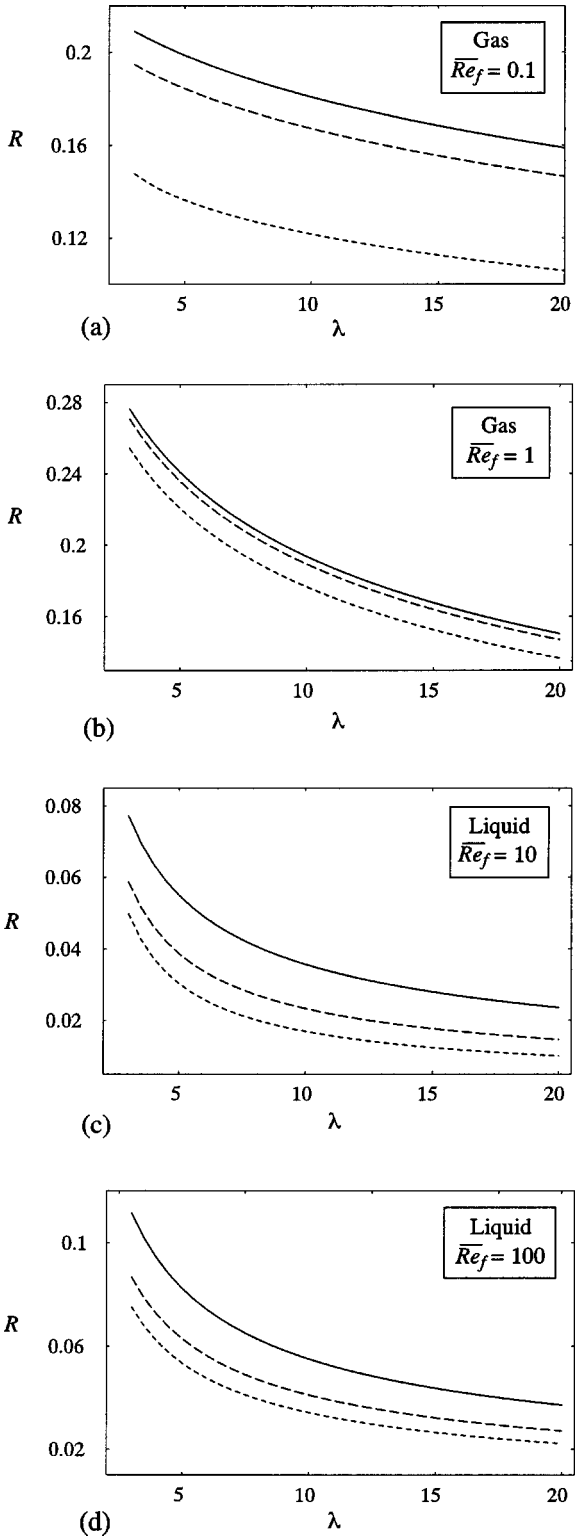

FIG. 9. Ratio of peak noise levels of torsional and flexural vibration, $R=(1+\nu)P(1|\omega_p^t)/F(1|\omega_p^f)$, where ω_p^t and ω_p^f refer to the fundamental peak frequencies of the torsional and flexural modes, respectively. Gas: (a) $\overline{\mathrm{Re}_f}=0.1$; (b) $\overline{\mathrm{Re}_f}=1$; {$\overline{T}=0.005$ (——); $\overline{T}=0.015$ (— —); and $\overline{T}=0.045$ (– – –)}. Liquid: (c) $\overline{\mathrm{Re}_f}=10$; (d) $\overline{\mathrm{Re}_f}=100$; {$\overline{T}=5$ (——); $\overline{T}=15$ (— —); and $\overline{T}=45$ (– – –)}.

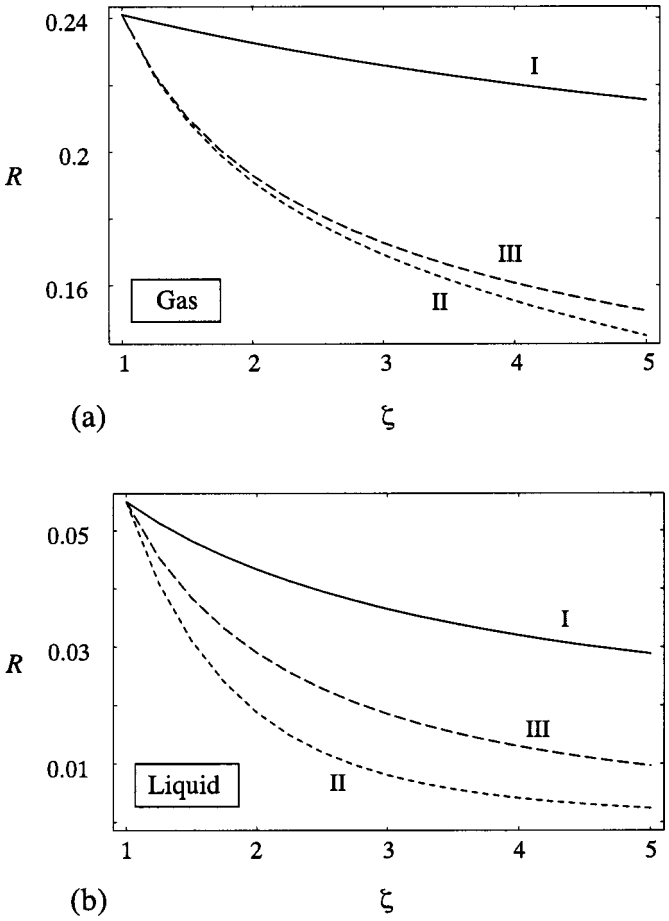

FIG. 10. Ratio of peak noise level of torsional and flexural vibration, $R=(1+\nu)P(1|\omega_p^t)/F(1|\omega_p^f)$ as a function of the geometric scaling parameter ζ, where ω_p^t and ω_p^f refer to the fundamental peak frequencies of the torsional and flexural modes, respectively. Case I (——); Case II (– – –); and Case III (— —). (a) Gas: At $\zeta=1$, we have $\overline{\mathrm{Re}_f}=1$, $\bar{T}=0.005$, and $\lambda=5$. (b) Liquid: At $\zeta=1$, we have $\overline{\mathrm{Re}_f}=10$, $\bar{T}=5$, and $\lambda=5$.

As an example, we consider a cantilever immersed in gas and liquid, that is characterized by the following initial ($\zeta=1$) parameter set: Gas ($\lambda=5$, $\overline{\mathrm{Re}_f}=1$, and $\bar{T}=0.005$); Liquid ($\lambda=5$, $\overline{\mathrm{Re}_f}=10$, and $\bar{T}=5$). We remind the reader that λ is independent of the medium in which the cantilever is immersed, and that $\overline{\mathrm{Re}}=\lambda\overline{\mathrm{Re}_f}$. We then vary the dimensions of the cantilever in accordance with the above three cases, i.e., we increase the geometric parameter ζ, and examine the ratio of the fundamental peak noise levels of torsional to flexural vibrations. The results of this study are given in Fig. 10, where we find that the ratio of the peak noise levels of torsional to flexural vibration decreases always. However, the rate at which this decrease occurs, and the mechanisms involved, differ in all three cases, the reasons for which shall now be discussed. We consider the case of immersion in gas in detail first.

In Case I, the ratio of the torsional and flexural vacuum frequencies is independent of ζ, see Eq. (46). Therefore, the fundamental peak frequencies of torsional and flexural vibrations in gas are approximately fixed relative to one another. In addition, both $\overline{\mathrm{Re}}$ and $\overline{\mathrm{Re}_f}$ decrease at the same rate with increasing ζ, namely, inversely proportional to ζ. Comparing Fig. 7(a) of this article and Fig. 6(a) of Ref. 3, we then observe that the ratio of the quality factor Q_t for the torsional response to the quality factor Q_f for the flexural response, is approximately constant as ζ is increased; the ratio of quality factors Q_t/Q_f decreases by $\sim$10% as ζ is increased from $\zeta=1$ to $\zeta=5$. This indicates that the torsional resonance peak flattens only slightly faster than the flexural peak with increasing ζ. Since the total thermal noise in the torsional mode relative to the flexural mode is fixed, it then follows that the ratio of the torsional peak noise level to the flexural peak noise level decreases by a small amount ($\sim$10%), see Fig. 10(a).

Next, we consider Case II. We find from Eq. (45) and (38) of Ref. 3, that $\overline{\mathrm{Re}}$ and $\overline{\mathrm{Re}_f}$ are inversely proportional to ζ and ζ^2, respectively. Thus, the quality factor Q_f for the fundamental flexural resonance decreases faster than the quality factor Q_t for the torsional resonance peak, causing the ratio Q_t/Q_f to increase significantly (by a factor of 2.06 as ζ increases from $\zeta=1$ to $\zeta=5$). This effect alone would cause the torsional peak noise level to increase relative to the flexural peak noise level. However, in addition to this effect, we observe from Eq. (46) that the ratio of torsional to flexural vacuum frequencies increases linearly with ζ. From this latter observation, it follows that as the torsional resonance peak shifts to higher frequencies relative to the flexural peak, the relative peak noise level of the torsional resonance will tend to decrease. This competing effect dominates the above quality factor effect, leading to a significant reduction in the ratio of the peak noise levels, as demonstrated in Fig. 10(a).

Case III is similar to Case II above. Again, from Eq. (45) and Eq. (38) of Ref. 3, we find that $\overline{\mathrm{Re}}$ and $\overline{\mathrm{Re}_f}$ are inversely proportional to ζ and ζ^2, respectively. Similarly, the ratio of torsional to flexural vacuum frequencies again increases linearly with ζ. For Case III, however, we also find that T is inversely proportional to ζ. This variation in T has the effect of modifying the quality factor for both the torsional and flexural resonance peaks, increasing the ratio of quality factor Q_t/Q_f to be greater than that observed in Case II (the ratio now increases by a factor of 2.15 as ζ is increased from $\zeta=1$ to $\zeta=5$). As in Case II, the effect of increasing the torsional resonance peak relative to the flexural resonance peak dominates the quality factor effect. However, since the ratio of the quality factors is slightly larger for Case III than for Case II , the decrease in the ratio of peak noise levels for Case III is slightly less than for Case II, as is observed in Fig. 10(a).

Similar trends to those in gases are observed for a cantilever immersed in liquid, see Fig. 10(b). Interestingly, however, the ratio of the peak noise levels is significantly smaller than the corresponding result in gas. This phenomenon can be understood by first noting that the peak noise level of the fundamental flexural mode in liquid is near its minimum value for the values of $\overline{\mathrm{Re}_f}$ considered. This is certainly not true for the fundamental flexural mode in gas, where the peak noise level greatly exceeds its minimum value. This is because the quality factor of the cantilever in liquid is near unity, whereas in gas the quality factor greatly exceeds unity, see Figs. 6 and 7 of Ref. 3. For the fundamental torsional mode, however, the quality factor in both gas and liquid is

greater than unity, indicating that the peak noise levels in both mediums exceed their minimum values, see Figs. 7 and 8. This indicates that the decrease in the peak noise level for the fundamental torsional mode is greater than that for the fundamental flexural mode as the cantilever moves from gas to liquid. It then follows that the ratio of the peak noise levels of torsional to flexural vibrations will be smaller in liquid than in gas.

In summary, we find that the fundamental torsional peak noise level is an order of magnitude smaller than the fundamental flexural peak noise level for immersion in gas, whereas in liquid, this difference increases to two orders of magnitude.

V. CONCLUSIONS

We have presented a general theoretical model for the frequency response of a cantilever beam executing torsional vibration in a viscous fluid. This model is applicable to a cantilever beam of arbitrary cross section that is excited by an arbitrary driving torque, and immersed in a fluid of arbitrary viscosity and density. the principal assumptions implemented in its formulation are that the cantilever length greatly exceeds its width, the amplitude of vibration is small, and the fluid is incompressible in nature. All these assumptions are typically satisfied in practice.

The model presented here complements and extends the previous formulation of Sader,[3] which was derived explicitly for a cantilever beam undergoing flexural vibration in a viscous fluid. The main findings of this study are commensurate with those of Ref. 3. In particular, it was found that fluid viscosity becomes increasingly important as the dimensions of the cantilever are reduced. For AFM cantilevers, this can have a dramatic effect on the torsional frequency response. In addition, the analogy with the response of a SHO for torsional vibrations was examined, and found to be valid when dissipative effects in the fluid are small, in line with the finding for flexural vibrations.

Due to its significance to AFM measurements, the case of a cantilever excited by a thermal driving force was studied in detail and explicit formulas and numerical results were presented for the thermal noise spectrum. In so doing, the relationship between the thermal noise spectra due to flexural and torsional vibrations was also examined. Most significantly, it was found that the peak noise levels of torsional vibrations are at least an order of magnitude smaller than those of flexural vibrations.

Finally, we note that combination of the results presented in this article with those in Ref. 3 enables the combined frequency response due to flexural and torsional motion to be calculated. Since no other motion can be detected using the AFM normally, this then enables the complete frequency response of AFM cantilever beams to be calculated. This can be done in an *a priori* fashion, from knowledge of the material and geometric properties of the cantilever and the viscosity and density of the fluid. These results are therefore expected to be of significant value to the design and application of AFM cantilever beams.

ACKNOWLEDGMENTS

This research was supported by the Particulate Fluids Processing Center of the Australian Research Council and the Australian Research Council Grants Scheme. C.P.G. gratefully acknowledges the support of an Australian Postgraduate Award.

APPENDIX A

In this Appendix, the hydrodynamic load on an infinitely thin and infinitely long rigid beam (i.e., a flat blade), that is immersed in a viscous fluid and executing infinitesimally small torsional oscillations about its major axis, is calculated numerically. This is performed using the boundary integral formulation of Tuck.[27] Since this special case was not considered explicitly in Ref. 27, a brief outline of the analysis is given here.

For such a beam, the normal component of the velocity at its surface is given by $V(y,t)=\Omega_0 y e^{-i\omega t}$, where Ω_0 is the angular velocity, whereas the tangential component of the surface velocity is zero. The coordinate system is as described in Fig. 1.

Tuck[27] showed that the Fourier-transformed Navier–Stokes and continuity equations can be recast formally into the following integral equation for the pressure difference Δp between top and bottom surfaces of the beam,

$$\int_{-1}^{1} \Delta P(\xi) L(-i\sqrt{i\ \mathrm{Re}}|\xi-\xi'|)d\xi=\xi', \tag{A1}$$

where $\Delta P(\xi)=\eta\Omega_0\Delta p(y)$ is the dimensionless pressure difference, $\xi=2y/b$, Re is the Reynolds number as given in Eq. (2), and the kernel function $L(z)$, is defined by

$$L(z)=-\frac{1}{2\pi}\frac{d^2}{dz^2}[\ln(z)+K_0(z)], \tag{A2}$$

where K_0 is a modified Bessel function of the third kind.[26] We outline the method of solution for Eq. (A1) below.

The hydrodynamic torque per unit length, M_{hydro}, acting on the beam can be determined, once $\Delta P(\xi)$ is known, using the following expression:

$$M_{\mathrm{hydro}}=-\frac{\eta\Omega_0 b^2}{4}\int_{-1}^{1}\Delta P(\xi)\xi d\xi. \tag{A3}$$

To calculate the hydrodynamic function $\Gamma(\omega)$, we refer to Eq. (9), from which we obtain the following normalization:

$$M_{\mathrm{hydro}}=-\frac{\pi}{8}i\omega\rho b^4\Omega_0\Gamma(\omega). \tag{A4}$$

Equating Eqs. (A3) and (A4) then gives the required expression for the hydrodynamic function in terms of the dimensionless pressure difference $\Delta P(\xi)$

$$\Gamma(\omega)=\frac{1}{2\pi i\ \mathrm{Re}}\int_{-1}^{1}\Delta P(\xi)\xi d\xi. \tag{A5}$$

Equation (A1) was solved for $\Delta P(\xi)$ using the numerical quadrature scheme described in Ref. 27; this recast Eq. (A1) into a system of linear equations which were then solved using matrix techniques. The numerical solution for

$\Delta P(\xi)$ was then substituted into Eq. (A5) to obtain the required hydrodynamic function $\Gamma(\omega)$, the numerical results of which are given in Fig. 3.

We note that the hydrodynamic function of a beam of arbitrary cross section can be computer using the general technique developed by Tuck.[27]

APPENDIX B

We now calculate the low and high Reynolds number asymptotic behavior of the hydrodynamic function, $\Gamma(\omega)$, i.e., $\mathrm{Re}\to 0$ and $\mathrm{Re}\to\infty$, respectively.

1. Low Reynolds number limit (Re→0)

In the limit as $\mathrm{Re}\to 0$, the kernel of Eq. (A1) can be expanded formally to give[26]

$$L(-i\sqrt{i\,\mathrm{Re}}|\xi-\xi'|)=\frac{1}{4\pi}\{\ln|\xi-\xi'|+C_1 - i\,\mathrm{Re}(\xi-\xi')^2(\tfrac{3}{8}\ln|\xi-\xi'|+C_2)\}+O[\mathrm{Re}^4\ln(Re)], \tag{B1}$$

where C_1 and C_2 are defined as

$$C_1=\ln(-i\sqrt{i\,\mathrm{Re}})+\tfrac{1}{2}+\gamma-\ln(2),\qquad C_2=\tfrac{3}{8}\ln(-i\sqrt{i\,\mathrm{Re}})-\tfrac{11}{32}+\tfrac{3\gamma}{8}-\tfrac{3}{8}\ln(2), \tag{B2}$$

and γ is the Euler constant.[26] Next, we expand the pressure as

$$P(\xi)=P_0(\xi)+\mathrm{Re}P_1(\xi)+\cdots. \tag{B3}$$

Substituting Eqs. (B2) and (B3) into Eq. (A1), and equating terms of equal order in Re, gives the following $O(1)$ integral equation:

$$\int_{-1}^{1}P_0(\xi)(\ln|\xi-\xi'|+C_1)d\xi=4\pi\xi', \tag{B4}$$

and $O(\mathrm{Re})$ equation,

$$\int_{-1}^{1}P_1(\xi)(\ln|\xi-\xi'|+C_1)d\xi = i\int_{-1}^{1}P_0(\xi)(\xi-\xi')^2(\tfrac{3}{8}\ln|\xi-\xi'|+C_2)d\xi. \tag{B5}$$

Differentiating Eq. (B4) with respect to ξ', we obtain

$$\int_{-1}^{1}\frac{P_0(\xi)}{\xi-\xi'}d\xi=-4\pi, \tag{B6}$$

which has the following exact solution[32]

$$P_0(\xi)=-\frac{4\xi}{\sqrt{1-\xi^2}}. \tag{B7}$$

Differentiating Eq. (B5) with respect to ξ', and using Eq. (B7), we find that the exact solution to the $O(\mathrm{Re})$ integral equation is[32]

$$P_1(\xi)=-\frac{4iC_2\xi}{\sqrt{1-\xi^2}}. \tag{B8}$$

Hence, we obtain the following expression for the pressure distribution as $\mathrm{Re}\to 0$:

$$P(\xi)=-\frac{4\xi}{\sqrt{1-\xi^2}}(1+i\ \mathrm{Re}\ C_2+\cdots). \tag{B9}$$

Substituting Eqs. (B2) and (B9) into Eq. (A5) gives the required low-frequency asymptote of the hydrodynamic function, as $\mathrm{Re}\to 0$

$$\Gamma(\omega)=\frac{i}{\mathrm{Re}}-\frac{3}{8}\ln(-i\sqrt{i\ \mathrm{Re}}),\quad \mathrm{Re}\to 0. \tag{B10}$$

2. High Reynolds number limit (Re→∞)

The limit as $\mathrm{Re}\to\infty$ corresponds to immersion in an inviscid fluid. In this case, we expect the pressure to be continuous at the edges of the beam and antisymmetric over its top and bottom faces. We therefore seek a solution to Eq. (A1) that satisfies the condition $P(\pm 1)=0$.

As $\mathrm{Re}\to\infty$, the kernel of Eq. (A1) can be expanded to give[26]

$$L(-i\sqrt{i\ \mathrm{Re}}|\xi-\xi'|)=-\frac{1}{2\pi\ i\mathrm{Re}(\xi-\xi')^2}+O(\mathrm{Re}^{-1/4}e^{-\sqrt{\mathrm{Re}}}). \tag{B11}$$

Substituting Eq. (B11) into Eq. (A1), we then obtain

$$\int_{-1}^{1}\frac{P(\xi)}{(\xi-\xi')^2}d\xi=-2\pi i\ \mathrm{Re}\ \xi'. \tag{B12}$$

Integrating by parts and using the property that $P(\pm 1)=0$, we find

$$\int_{-1}^{1}\frac{P'(\xi)}{\xi-\xi'}d\xi=-2\pi i\ \mathrm{Re}\ \xi', \tag{B13}$$

which has the bound solution[32]

$$P(\xi)=i\ \mathrm{Re}\ \xi\sqrt{1-\xi^2}. \tag{B14}$$

Substituting Eq. (B14) into Eq. (A5) then gives the high-frequency asymptote of the hydrodynamic function as $\mathrm{Re}\to\infty$.

$$\Gamma(\omega)=\frac{1}{16},\quad \mathrm{Re}\to\infty. \tag{B15}$$

In addition, we expect the boundary layer in this high-Re limit to contribute a term to $\Gamma(\omega)$ which behaves like $iC/\sqrt{\mathrm{Re}}$, where C is some real constant. In principle, this constant could be obtained by taking higher-order terms in the expansion of the kernel, Eq. (B11), and using integral transform techniques.[33] Rather than formally deriving this constant using this approach, which poses a formidable challenge, we use a simple nonlinear least-squares fitting algorithm on the imaginary component of the high-Re numerical data, which suggests $C\approx 0.41$. This value is used in formulating the empirical expression for the hydrodynamic function, Eq. (21).

[1] W.-H. Chu, Technical Report No. 2, DTMB, Contract NObs-86396(X), Southwest Research Institute, San Antonio, Texas, 1963.
[2] U.S. Lindholm, D. D. Kana, W.-H. Chu, and H. N. Abramson, J. Ship Res. **9**, 11 (1965).

[3] J. E. Sader, J. Appl. Phys. **84**, 64 (1998).
[4] L. Landweber, J. Ship Res. **11**, 143 (1967).
[5] G. Y. Chen, R. J. Warmack, T. Thundat, D. P. Allison, and A. Huang, Rev. Sci. Instrum. **65**, 2532 (1994).
[6] T. E. Schäffer, J. P. Cleveland, F. Ohnesorge, D. A. Walters, and P. K. Hansma, J. Appl. Phys. **80**, 3622 (1996).
[7] F.-J. Elmer and M. Dreier, J. Appl. Phys. **81**, 7709 (1997).
[8] D. A. Walters, J. P. Cleveland, N. H. Thomson, P. K. Hansma, M. A. Wendman, G. Gurley, and V. Elings, Rev. Sci. Instrum. **67**, 3583 (1996).
[9] H.-J. Butt, P. Siedle, K. Seifert, K. Fendler, T. Seeger, E. Bamberg, A. Weisenhorn, K. Goldie, and A. Engel, J. Microsc. **169**, 75 (1993).
[10] M. V. Salapaka, H. S. Bergh, J. Lai, A. Majumdar, and E. McFarland, J. Appl. Phys. **81**, 2480 (1997).
[11] J. W. M. Chon, P. Mulvaney, and J. E. Sader, J. Appl. Phys. **87**, 3978 (2000).
[12] L. D. Landau and E. M. Lifshitz, *Theory of Elasticity* (Pergamon, London, 1959).
[13] J. E. Sader, J. W. M. Chon, and P. Mulvaney, Rev. Sci. Instrum. **70**, 3967 (1999).
[14] G. Behme and T. Hesjedal, J. Appl. Phys. **89**, 4850 (2001).
[15] G. Bogdanovic, A. Meurk, and M. W. Rutland, Colloids Surf., B **19**, 397 (2000).
[16] G. Behme, T. Hesjedal, E. Chilla, and H.-J. Frölich, Appl. Phys. Lett. **73**, 882 (1998).
[17] S. Timoshenko, D. H. Young, and W. Weaver, *Vibration Problems in Engineering* (Wiley, New York, 1974). We only consider the case where coupling between flexural and torsional vibrations is negligible.
[18] H.-J. Butt and M. Jaschke, Nanotechnology **6**, 1 (1995).
[19] This condition also holds for cantilevers composed of crystalline materials, provided the crystal orientation is fixed along the entire length of the cantilever.
[20] This can also be satisfied for cantilevers with sharp edges, since the radius of curvature of such edges is always greater than zero in practice.
[21] The convention adopted for the Reynolds number conforms with Ref. 30. We note that the Reynolds number is often associated with the nonlinear convective inertial term of the Navier–Stokes equation. This latter convention has not been adopted here.
[22] R. J. Roark, *Formulas for Stress and Strain* (McGraw-Hill, New York, 1943).
[23] The product *GK* is commonly referred to as the torsional rigidity of the beam.
[24] P. M. Morse and H. Feshbach, *Methods of Theoretical Physics* (McGraw-Hill, New York, 1953).
[25] G. G. Stokes Math. Phys. Pap. **5**, 207 (1886).
[26] M. Abramowitz and I. A. Stegun, *Handbook of Mathematical Functions* (Dover, New York, 1972).
[27] E. O. Tuck, J. Eng. Math. **3**, 29 (1969).
[28] Note that the undamped modes for flexural vibration presented in Ref. 3 form an orthonormal, rather than orthogonal basis set.
[29] A. E. H. Love, *A Treatise on the Mathematical Theory of Elasticity* (Pergamon, London, 1959).
[30] G. K. Batchelor, *An Introduction to Fluid Dynamics* (Cambridge University, Cambridge, England, 1974).
[31] This is typically satisfied if the laser spot is positioned at the center of the quadrant in the split photodiode.
[32] A. D. Polyanin and A. V. Manzhirov, *Handbook of Integral Equations* (CRC, Boca Raton, 1998).
[33] H. Hochstadt, *Integral Equations* (Wiley, New York, 1973).